役割としては，TGF-βをはじめとする液性因子のほか，細胞外マトリックスの供給が考えられた．そこでマイクロアレイ解析を行いM15細胞ではラミニンα5の発現が高いことを明らかにするとともに，これらラミニンの強制発現株を使った疑似基底膜でもM15細胞と同様な肝細胞誘導効果を確認した[17,18]．

最近，八木・北川により，脱細胞化したブタ肝臓に肝細胞を灌流することで類洞構造をもった組織を再構築できることが報告され[19]，組織3次元構築にも細胞外マトリックスなどの細胞周囲微小環境の重要性が改めて示された．

Ⅶ 移植細胞の効果と分化度

損傷の治癒機転として，構成細胞の自己複製あるいは体性(組織)幹細胞の導入，あるいはほかの種類の構成細胞が分化転換するなどして，失われた機能を取り戻そうとする一方で，細胞外マトリックスの産生や線維化といった臓器の3次元的な再構築(リモデリング)が行われる．移植細胞が担う役割としてはいまだ詳細は不明であるが，移植細胞が実質細胞へと分化するほかに，成長因子分泌などのパラクライン作用により宿主肝細胞やその前駆細胞の動員や血管形成に寄与する機序が想定されている[2,20]．

このほかに骨髄性幹細胞移植では，骨髄単核球による宿主肝細胞の細胞融合による効果も挙げられる[21,22]．他方で，細胞分化度が高いほど生着率が上昇することが報告されている[23]．多分化能あるいは分化転換能を有する細胞を移植する場合，奇形腫や肝腫瘍形成といった問題以外にも，肝星（伊東）細胞やKupffer細胞あるいは筋線維芽細胞といった肝線維化を促す非実質細胞へと分化してしまうリスクも考えられる[24]．これらの問題を打開するために，細胞膜上に存在する肝成熟化マーカーであるアシアロ糖タンパク受容体を使った細胞分取法[25]や，肝細胞と胆管細胞への両分化能だけを有する細胞をEpCAM（epithelial cell adhesion molecule；上皮細胞接着分子）で細胞分取する方法[26]などが開発されている．

このように種々の細胞群が移植候補として挙げられるが，これら移植される細胞がいかなる種類のどのような分化度の細胞が適しているかについては，いまだ議論の余地がある．

Ⅷ 本邦での肝再生医療とヒト幹細胞臨床研究

1986年に劇症肝炎患者から単離されたHGFは，その後，報告者の1人である坪内らによって2005年9月から2008年6月まで第I/II相臨床試験が行われた[27]．坂井田らによって自己骨髄細胞投与がC型やB型肝炎ウイルスに起因する肝硬変患者やアルコール性肝硬変患者で有効であったと報告されている[28]．

2012年9月19日発表の厚生労働省発表の資料によれば，わが国で承認されている臨床試験として，先に述べた山口大学での「C型肝炎ウイルスに起因する肝硬変患者に対する自己骨髄細胞投与療法の有効性と安全性に関する研究」(2015年3月まで)や，金沢大学での「肝硬変に対する自己脂肪組織由来間質細胞の経肝動脈投与による肝再生療法の研究」(2015年8月まで）が実施中である．

おわりに

本邦でヒトiPS細胞が樹立され5年が経ち，分化誘導した色素上皮細胞のヒトへの移植が承認され，新たな局面を迎えている．このような状況において，神経などの外胚葉系組織や心筋などの中胚葉系組織に比べ，肝細胞や膵β細胞などの内胚葉系組織の分化誘導研究は遅れをとっている．また，最終的な目標である臨床応用へは，先に述べたドナーからの新鮮な肝細胞移植と同様の問題に直面する可能性が考えられる．これらに対して生体工学的なアプローチから研究が進められており，集学的に解決されることが待望される．

文　献

1) Hughes RD, Mitry RR, Dhawan A : Current status of hepatocyte transplantation. *Transplantation* 2012 ; 93 : 342–347.
2) Li J, Li M, Niu B, *et al* : Therapeutic potential of stem cell in liver regeneration. *Front Med* 2011 ; 5 : 26–32.
3) Lee KD, Kuo TK, Whang-Peng J, *et al* : In vitro hepatic differentiation of human mesenchymal stem cells. *Hepatology* 2004 ; 40 : 1275–1284.
4) Kakinuma S, Tanaka Y, Chinzei R, *et al* : Human umbilical cord blood as a source of transplantable hepatic progenitor cells. *Stem Cells* 2003 ; 21 : 217–227.
5) Mitaka T : Hepatic stem cells : from bone marrow cells to hepatocytes. *Biochem Biophys Res Commun* 2001 ; 281 : 1–5.
6) Kuwahara R, Kofman AV, Landis CS, *et al* : The hepatic stem cell niche : identification by label-retaining cell assay. *Hepatology* 2008 ; 47 : 1994–2002.
7) Lowes KN, Brennan BA, Yeoh GC, *et al* : Oval cell numbers in human chronic liver diseases are directly related to disease severity. *Am J Pathol* 1999 ; 154 : 537–541.
8) Xiao JC, Jin XL, Ruck P, *et al* : Hepatic progenitor cells in human liver cirrhosis : immunohistochemical, electron microscopic and immunofluorencence confocal microscopic findings. *World J Gastroenterol* 2004 ; 10 : 1208–1211.
9) Libbrecht L, Desmet V, Van Damme B, *et al* : Deep intralobular extension of human hepatic 'progenitor cells' correlates with parenchymal inflammation in chronic viral hepatitis : can 'progenitor cells' migrate? *J Pathol* 2000 ; 192 : 373–378.
10) Baddour JA, Sousounis K, Tsonis PA : Organ repair and regeneration : an overview. *Birth Defects Res C Embryo Today* 2012 ; 96 : 1–29.
11) Sekiya S, Suzuki A : Direct conversion of mouse fibroblasts to hepatocyte-like cells by defined factors. *Nature* 2011 ; 475 : 390–393.
12) Rambhatla L, Chiu CP, Kundu P, *et al* : Generation of hepatocyte-like cells from human embryonic stem cells. *Cell Transplant* 2003 ; 12 : 1–11.
13) Shiraki N, Umeda K, Sakashita N, *et al* : Differentiation of mouse and human embryonic stem cells into hepatic lineages. *Genes Cells* 2008 ; 13 : 731–746.
14) Shiraki N, Yoshida T, Araki K, *et al* : Guided differentiation of embryonic stem cells into Pdx1-expressing regional-specific definitive endoderm. *Stem Cells* 2008 ; 26 : 874–885.
15) Shiraki N, Higuchi Y, Harada S, *et al* : Differentiation and characterization of embryonic stem cells into three germ layers. *Biochem Biophys Res Commun* 2009 ; 381 : 694–699.
16) Umeda K, Suzuki K, Yamazoe T, *et al* : Albumin gene targeting in human embryonic stem cells and induced pluripotent stem cells with helper-dependent adenoviral vector to monitor hepatic differentiation. *Stem Cell Res* 2012 ; 10 : 179–194.
17) Shiraki N, Yamazoe T, Qin Z, *et al* : Efficient differentiation of embryonic stem cells into hepatic cells *in vitro* using a feeder-free basement membrane substratum. *PLoS One* 2011 ; 6 : e24228.
18) Higuchi Y, Shiraki N, Yamane K, *et al* : Synthesized basement membranes direct the differentiation of mouse embryonic stem cells into pancreatic lineages. *J Cell Sci* 2010 ; 123(Pt 16) : 2733–2742.
19) 八木　洋，北川雄光：脱細胞化技術を用いた新しい再生療法．日外会誌 2012 ; 113 : 419–423.
20) Parekkadan B, van Poll D, Suganuma K, *et al* : Mesenchymal stem cell-derived molecules reverse fulminant hepatic failure. *PLoS One* 2007 ; 2 : e941.
21) Willenbring H, Bailey AS, Foster M, *et al* : Myelomonocytic cells are sufficient for therapeutic cell fusion in liver. *Nat Med* 2004 ; 10 : 744–748.
22) Camargo FD, Finegold M, Goodell MA : Hematopoietic myelomonocytic cells are the major source of hepatocyte fusion partners. *J Clin Invest* 2004 ; 113 : 1266–1270.
23) Haridass D, Yuan Q, Becker PD, *et al* : Repopulation efficiencies of adult hepatocytes, fetal liver progenitor cells, and embryonic stem cell-derived hepatic cells in albumin-promoter-enhancer urokinase-type plasminogen activator mice. *Am J Pathol* 2009 ; 175 : 1483–1492.
24) Greenbaum LE, Wells RG : The role of stem cells in liver repair and fibrosis. *Int J Biochem Cell Biol* 2011 ; 43 : 222–229.
25) Basma H, Soto-Gutiérrez A, Yannam GR, *et al* : Differentiation and transplantation of human embryonic stem cell-derived hepatocytes. *Gastroenterology* 2009 ; 136 : 990–999.
26) Okabe M, Tsukahara Y, Tanaka M, *et al* : Potential hepatic stem cells reside in EpCAM+ cells of normal and injured mouse liver. *Development* 2009 ; 136 : 1951–1960.
27) Ido A, Moriuchi A, Numata M, *et al* : Safety and pharmacokinetics of recombinant human hepatocyte growth factor (rh-HGF) in patients with fulminant hepatitis : a phase I/II clinical trial, following preclinical studies to ensure safety. *J Transl Med* 2011 ; 9 : 55.
28) 坂井田功：肝硬変に対する自己骨髄細胞投与療法の現状と展望．臨病理 2011 ; 59 : 1092–1098.

nature chemical biology

ARTICLE

PUBLISHED ONLINE: 15 DECEMBER 2013 | DOI: 10.1038/NCHEMBIO.1410

VMAT2 identified as a regulator of late-stage β-cell differentiation

Daisuke Sakano[1], Nobuaki Shiraki[1], Kazuhide Kikawa[1,2], Taiji Yamazoe[1], Masateru Kataoka[1], Kahoko Umeda[1], Kimi Araki[3], Di Mao[4], Shirou Matsumoto[2], Naomi Nakagata[5], Olov Andersson[6,7], Didier Stainier[6,8], Fumio Endo[2], Kazuhiko Kume[1,10], Motonari Uesugi[4] & Shoen Kume[1,9]*

Cell replacement therapy for diabetes mellitus requires cost-effective generation of high-quality, insulin-producing, pancreatic β cells from pluripotent stem cells. Development of this technique has been hampered by a lack of knowledge of the molecular mechanisms underlying β-cell differentiation. The present study identified reserpine and tetrabenazine (TBZ), both vesicular monoamine transporter 2 (VMAT2) inhibitors, as promoters of late-stage differentiation of *Pdx1*-positive pancreatic progenitor cells into *Neurog3* (referred to henceforth as *Ngn3*)-positive endocrine precursors. VMAT2-controlled monoamines, such as dopamine, histamine and serotonin, negatively regulated β-cell differentiation. Reserpine or TBZ acted additively with dibutyryl adenosine 3′,5′-cyclic AMP, a cell-permeable cAMP analog, to potentiate differentiation of embryonic stem (ES) cells into β cells that exhibited glucose-stimulated insulin secretion. When ES cell-derived β cells were transplanted into AKITA diabetic mice, the cells reversed hyperglycemia. Our protocol provides a basis for the understanding of β-cell differentiation and its application to a cost-effective production of functional β cells for cell therapy.

© 2014 Nature America, Inc. All rights reserved.

npg

Pancreatic cells arise from definitive endoderm and Pdx1-positive (Pdx1+) pancreatic progenitor cells[1], which proliferate and give rise to all three pancreatic lineages: acini, ducts and endocrine islets[2]. Endocrine precursors are characterized by the transient expression of the basic helix-loop-helix transcription factor neurogenin 3 (Ngn3, also known as Neurog3)[2]. Previous studies showed that Ngn3 specifically establishes the endocrine lineages and that loss of Ngn3 precludes endocrine cell development[2,3]. Production of islet cells occurs through the concerted activation of a combination of transcription factors[4]. However, the coordination of cell fate decisions remains poorly understood.

The prevalence of diabetes mellitus in many populations is high, and development of cell replacement therapy through generation of β cells from ES cells is a research priority. Recent studies have shown that mouse or human ES cells can be induced to recapitulate embryonic development of the pancreas[5]. Studies on ES cell differentiation into endodermal or pancreatic cell lineages have shown that stimulation with activin, FGF or retinoic acid, in addition to inhibition of hedgehog signaling by KAAD-cyclopamine, promotes the differentiation into endoderm or pancreatic fates[6,7]. New signal pathways that promote ES cell differentiation into endodermal[8] or pancreatic[9] lineages have been discovered through large-scale screening of cell-permeable, bioactive small molecules. However, it is still difficult to derive mature β cells that secrete insulin in a glucose-dependent manner. A better understanding is needed of the underlying molecular mechanisms that control the late stages of β-cell development, in which Pdx1+ pancreatic progenitor cells develop into Ngn3+ endocrine progenitor cells and insulin-positive (Ins+) β cells and then further differentiate into mature β cells capable of glucose-stimulated insulin secretion (GSIS).

Here, we identified reserpine and TBZ as potent promoters of pancreatic progenitor cell differentiation into functional β cells. This study highlights the use of chemical compound libraries for the identification of new developmental pathways that control progenitor cell differentiation into mature β cells.

RESULTS

Reserpine and TBZ increase Ins+ cells

The present study used large-scale screening of chemical compounds with an ES cell line, SK7, that expresses GFP under the *Pdx1* promoter[10,11]. The *Pdx1*-GFP ES cell line is useful because the expression of *Pdx1* is biphasic (**Fig. 1a**), which enabled the detection of early-stage Pdx1+ pancreatic progenitors and late-stage Pdx1+ Ins+ β cells . We optimized the culture to promote modest basal differentiation with high reproducibility, so that the markers *Sox17*, *Pdx1*, *Ngn3* and *Ins1* were sequentially expressed (**Fig. 1a**).

To screen for compounds that potentiate the differentiation of ES cell–derived Pdx1+ pancreatic progenitor cells into insulin-expressing cells, we tested a library of 1,120 biologically active compounds arrayed as single compounds in DMSO on cultures, starting on day 11 after confirming the appearance of *Pdx1*-GFP+ cells and conducting the assay on day 17 (**Fig. 1a**). Candidate compounds that increased both *Ins1* expression and the number of Ins+ cells relative to vehicle (1% DMSO) were selected as primary hits. The coefficient of variation of this screen was 0.36 ± 0.0447 (± s.d.), which was difficult to minimize further owing to the long assay

[1]Department of Stem Cell Biology, Institute of Molecular Embryology and Genetics, Kumamoto University, Kumamoto, Japan. [2]Department of Pediatrics, Graduate School of Medical Sciences, Kumamoto University, Kumamoto, Japan. [3]Laboratory of Developmental Genetics, Institute of Resource Development and Analysis, Kumamoto University, Kumamoto, Japan. [4]Institute for Chemical Research and Institute for Integrated Cell-Material Sciences, (WPI-iCeMS), Kyoto University, Kyoto, Japan. [5]Division of Reproductive Engineering, Center for Animal Resources and Development, Kumamoto University, Kumamoto, Japan. [6]Department of Cell and Molecular Biology, Karolinska Institute, Stockholm, Sweden. [7]Department of Biochemistry and Biophysics, University of California–San Francisco, San Francisco, California, USA. [8]Department of Developmental Genetics, Max Planck Institute for Heart and Lung Research, Bad Nauheim, Germany. [9]Program for Leading Graduate Schools, Health Life Science Interdisciplinary and Global Oriented (HIGO) Program, Kumamoto University, Kumamoto, Japan. [10]Present address: Department of Neuropharmacology, Graduate School of Pharmaceutical Sciences, Nagoya City University, Nagoya, Japan. *e-mail: skume@kumamoto-u.ac.jp

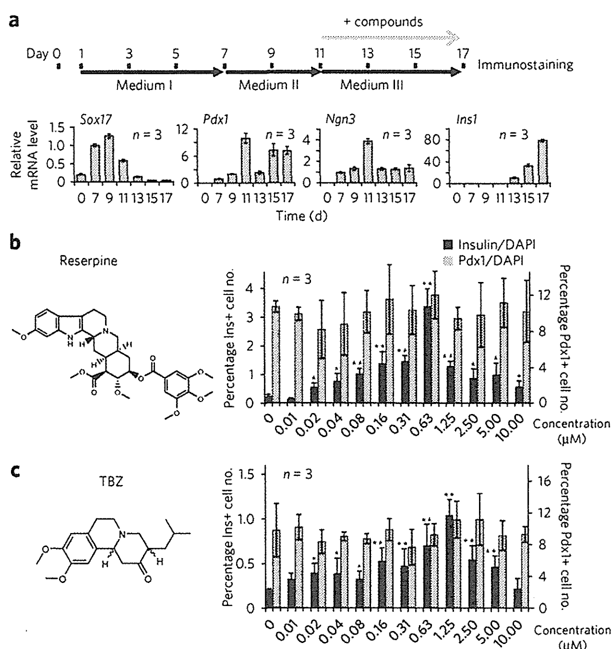

Figure 1 | Reserpine identified as a chemical that enhanced ES cell differentiation into pancreatic β cells. Using a high-throughput screening system, a chemical library was screened, and reserpine was identified as a hit chemical. (**a**) A high-throughput screening system for chemicals that enhance differentiation into β cells. Transcript expressions of *Sox17*, *Pdx1*, *Ngn3* and *Ins1* are expressed as fold change relative to control on day 7. (**b**,**c**) Reserpine (**b**) and TBZ (**c**) (chemical structure shown at left) increased the number of β cells relative to the total number of DAPI-stained cells (black bars) without affecting Pdx1+ cells (light gray bars). In **a**–**c**, data shown are mean ± s.d. ($n = 3$); significant differences between treatment and control at $^{*}P < 0.05$ and $^{**}P < 0.01$ are shown (two-tailed paired Student's t-test).

period. To overcome this, we investigated dose dependencies of the hit chemicals as a secondary screen. Of our hit compounds, the indole alkaloid antipsychotic and antihypertensive drug reserpine demonstrated the strongest effect. Reserpine increased the proportion of Ins+ cells in a concentration-dependent manner without altering the *Pdx1*-GFP+ cell ratio (**Fig. 1b**). Reserpine is known to deplete monoamines from secretory vesicles by blocking uptake into monoamine secretary granules, mediated by VMAT proteins[12–15]. Because human pancreatic β cells express the isoform VMAT2 (refs. 16–19), we also tested another VMAT2 inhibitor, TBZ, which also increased the amount of insulin-expressing cells in a dose-dependent manner (**Fig. 1c**). The half-maximal effective concentration (EC_{50}) values of reserpine and TBZ were 0.19 μM and 0.22 μM, respectively. The concentrations that led to 50% cell death (TD_{50}) were 1.56 μM reserpine and 5.98 μM TBZ. In a separate experiment, we treated cells with 0.63 μM reserpine or 1.25 μM TBZ (**Supplementary Results, Supplementary Fig. 1**). We confirmed the increases in the percentage of Ins+ cells out of the total cell numbers versus the untreated cells and in the relative *Ins1* mRNA levels (by real-time PCR) (**Supplementary Fig. 1**). These results suggested that VMAT2 is the candidate target molecule of reserpine and TBZ, which has a pivotal role in the differentiation of ES cells into Ins-expressing cells.

VMAT2 inhibited differentiation into Ins+ cells

To identify the role of VMAT2 in differentiation of ES cells into pancreatic β cells, we performed a knockdown of VMAT2. We established two VMAT2-knockdown SK7 cell lines, VMAT2KD1 and VMAT2KD2, using lentiviral short hairpin RNA (shRNA) (**Fig. 2a**). VMAT2KD2 exhibited lower *Slc18a2* (henceforth referred to as *Vmat2*) expression than VMAT2KD1 (**Fig. 2a**) and showed greater increases in the number of β cells and level of *Ins1* transcription (**Fig. 2b**). These results indicated that reserpine- or TBZ-mediated VMAT2 inhibition led to an enhancement of differentiation into Ins+ cells. Therefore, VMAT2-mediated monoamine storage functions as a negative regulator of differentiation into Ins+ cells. Pancreatic islets have an isozyme of the monoamine-catabolizing enzyme, monoamine oxidase B (MAO_B)[20]. We then tested the effects of application of pargyline, an MAO_B inhibitor (MAO_{Bi}), to stabilize the monoamines and increase intracellular monoamines. Indeed, application of pargyline had an inhibitory effect on the number of β cells and the level of *Ins1* expression, and reserpine counteracted the inhibitory effect of MAO_{Bi} (**Supplementary Fig. 2**). Moreover, the number and expression level of *Pdx1*-GFP+ cells was unaffected (**Supplementary Fig. 2**), similarly to treatment with reserpine and TBZ (**Fig. 1b,c**).

Monoamines such as dopamine, histamine and serotonin are known to be the substrates for VMAT2. We tested the effect of these monoamines by exogenous application and found that incubation with dopamine, histamine or serotonin from days 11–17 suppressed β-cell differentiation, with EC_{50} values of 1.25 μM (dopamine), 0.5 μM (histamine) and 0.92 μM (serotonin) (**Fig. 2c–e**). We determined the monoamine contents in the ES cell–derived cells on day 17 (**Fig. 2f–h** and **Supplementary Fig. 3a,b**). The dopamine content (approximately 1.3 pg/μg DNA) was approximately 100-fold higher compared to the other monoamines, whereas histamine was undetectable. Inhibition of VMAT2 with TBZ or reserpine and knockdown of *Vmat2* with shRNA significantly decreased ($P < 0.005$) monoamine contents, whereas treatment with pargyline increased it ($P < 0.01$) (**Fig. 2f,h** and **Supplementary Fig. 3**). The enzyme that synthesizes dopamine, tyrosine hydroxylase (Th), was expressed in the ES cells during differentiation at a level comparable to that in the embryonic pancreatic bud. By contrast, the histamine-synthesizing enzyme histidine decarboxylase (Hdc) and the serotonin-synthesizing enzyme tryptophan hydroxylase 1 (Tph1) were expressed at approximately 0.066-fold lower levels compared to those in the embryonic pancreas (**Supplementary Fig. 4a–c**). The monoamine receptors dopamine D2 (Drd2), histamine H1 (Hrh1), histamine H2 (Hrh2) and serotonin 1A (Htr1a) were expressed in day 11 and day 13 differentiated cells (**Supplementary Fig. 4d–f**). Upon addition of chemical compounds that inhibit the synthesizing enzymes for dopamine (α-methyl-tyrosine (α-MT) and L-3,4-dihydroxyphenylalanine (L-DOPA)), histamine (α-fluoromethylhistidine (α-FMH)) or serotonin (5-hydroxy tryptophan (5HTP) and carbidopa), we observed increases in Ins+ cell numbers (**Supplementary Fig. 4g–i**).

Taken together, VMAT2-controlled monoamine release exerted inhibitory effects on the differentiation of pancreatic progenitor cells into Ins+ cells. Reserpine and TBZ inhibit the uptake of monoamines into vesicular stores, which led to depletion of monoamines and potentiation of Ins+ cell differentiation.

TBZ increased differentiation into Ngn3+ cells

We then examined the effects of TBZ on marker expression in ES cell–derived cells by real-time PCR. We used TBZ instead of reserpine owing to its lower cytotoxicity; the results are expressed as fold changes compared to control treatments without chemicals at day 13. Treatment with TBZ resulted in a marked increase of *Ngn3*, *Nkx6-1* and *Ins1* transcripts on day 15 and day 17 (**Fig. 3a**). The real-time PCR results suggested that TBZ increases differentiation of ES cell–derived cells into *Ngn3*+ endocrine progenitors. To follow the transient increase of *Ngn3*+ endocrine precursors in living cells, we developed an NGP9 ES cell line from a transgenic mouse line bearing the *Ngn3*-promoter-driven eGFP transgene[21].

© 2014 Nature America, Inc. All rights reserved.

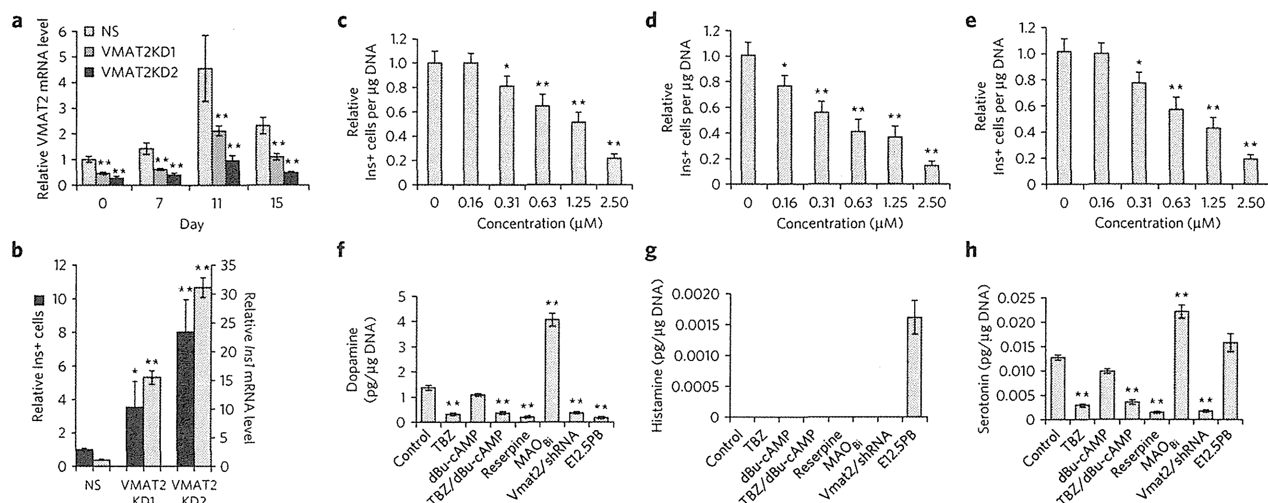

Figure 2 | VMAT2- and monoamine-dependent suppression of pancreatic β-cell differentiation. The effects of VMAT2- and monoamine-mediated inhibition on ES cell differentiation into Ins+ cells were tested, and monoamine cellular contents were determined. (a) Time-dependent expression of VMAT2 in VMAT2KD1 (dark gray), VMAT2KD2 (black) and control nonsilencing (NS; light gray) ES cell lines. (b) VMAT2KD1 and VMAT2KD2 ES cell lines yielded more Ins+ cells and *Ins1* transcripts than control NS ES cells. (c–e) Addition of monoamines, dopamine (c), histamine (d) or serotonin (e) suppressed differentiation of ES cells into Ins+ cells in a dose-dependent manner. (f–h) Cellular contents of dopamine (f), histamine (g) or serotonin (h) when added with VMAT2 inhibitors or MAO_{Bi}, treatment with both TBZ and dBu-cAMP. Control, no chemical treatment; MAO_{Bi}: 1 μM pargyline; Res: 0.63 μM reserpine; MAO_{Bi} + Res: 1 μM pargyline + 0.63 μM reserpine. For a–h, data shown are mean ± s.d. (n = 3); significant differences between treatment and no chemical treatment at *$P < 0.05$ and **$P < 0.01$ are shown (two-tailed paired Student's *t*-test). In a and b, black bars indicate Ins+ or *Pdx1*-GFP+ relative cell numbers, and gray bars indicate *Ins1* or *Pdx1* transcript expression relative to that in cells with no chemical treatment.

© 2014 Nature America, Inc. All rights reserved.

We treated the NGP9 cells with TBZ from day 11 to 13 and then performed the assay on day 13 (**Fig. 3b**). TBZ increased *Ngn3*-GFP+ cell numbers (**Fig. 3b**). These results indicate that VMAT2 signaling negatively controls differentiation into *Ngn3*-GFP+ endocrine precursors. We observed 5-ethynyl-2′-deoxyuridine (EdU) incorporation in Ngn3− cells but not in Ngn3+ cells, and TBZ addition did not increase EdU+ Ngn3+ cells, indicating that the increase in Ngn3+ cells was due to increased differentiation into Ngn3+ cells but not proliferation of Ngn3+ cells (**Fig. 3b** and **Supplementary Fig. 5a**). The Ngn3+ cells expressed Nkx2.2 and Nkx6.1 in their nuclei (**Supplementary Fig. 5b**).

We then examined whether this mechanism existed during normal embryonic development using an *in vitro* pancreas bud culture system. Upon addition of TBZ, we observed increased differentiation into insulin-, glucagon-, somatostatin- or pancreas polypeptide–expressing endocrine cells in the *Pdx1*-GFP+

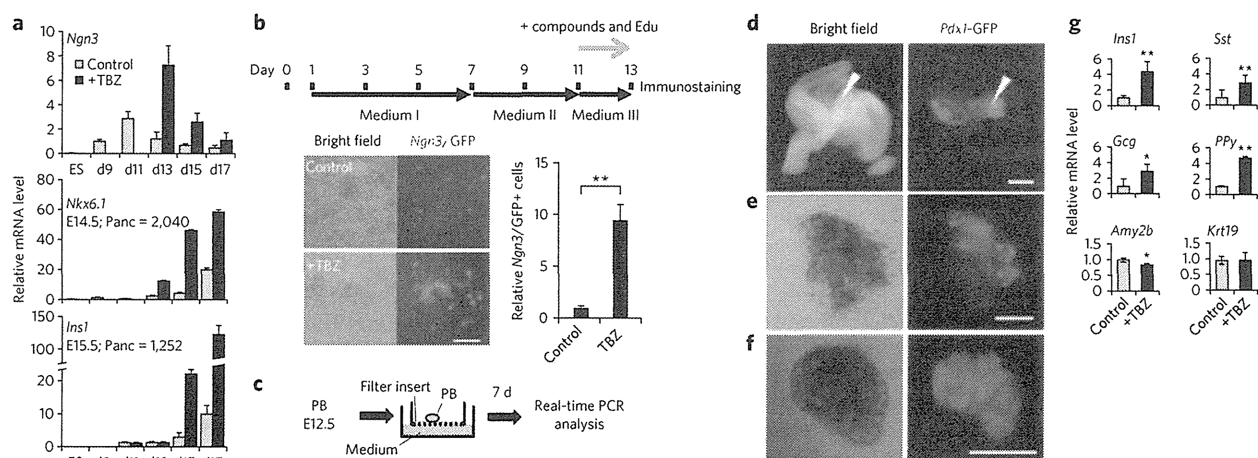

Figure 3 | VMAT2 inhibition increased differentiation into *Ngn3*-GFP+ cells. TBZ increased differentiation into *Ngn3*-GFP+ cells without increasing proliferation. (a) *Ngn3*, *Nkx6.1* and *Ins1* expression assayed on differentiation days (d) 13, 15 and 17, with or without (w/o) TBZ, expressed as fold change relative to control on day 13. Gray bars, no chemical (vehicle) samples; black bars, TBZ-treated samples. For all graphs, (n = 3). (b) A schematic drawing of the experimental design is shown. ES cell cultures were added with TBZ from day 11 to day 13 and assayed on day 13. Transmission or fluorescence images (left) and quantitative representations (right) of *Ngn3*-GFP+ cells without TBZ on day 13 are shown. (c) Schematic drawing of the experimental design. Pancreatic rudiments (PB, pancreatic bud) dissected from *Pdx1*-GFP mice at E12.5 were used for *ex vivo* culture for 7 d on filter inserts. (d–f) Transmission (left) and fluorescence (right) micrographs of explants before (d) and after culturing without TBZ (e; control DMSO) or with TBZ (f). (g) Semiquantitative real-time PCR was used to assay the expression of *Gcg*, *Sst*, *PPy*, *Amy2b* or *Krt19* after 7-d culture. Data shown are mean ± s.d. (n = 3), expressed as relative cell number compared to control. Scale bars, 200 μm. *$P < 0.05$ and **$P < 0.01$ (two-tailed paired Student's *t*-test).

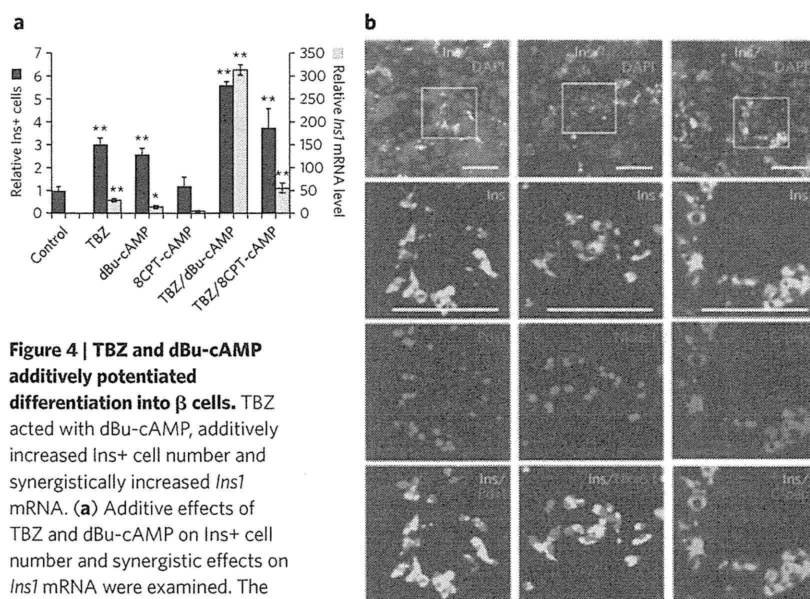

Figure 4 | TBZ and dBu-cAMP additively potentiated differentiation into β cells. TBZ acted with dBu-cAMP, additively increased Ins+ cell number and synergistically increased *Ins1* mRNA. (**a**) Additive effects of TBZ and dBu-cAMP on Ins+ cell number and synergistic effects on *Ins1* mRNA were examined. The results are expressed as fold change relative to control vehicle treatment (DMSO). By contrast, treatment with 8CPT-cAMP, a cAMP analog that specifically activates Epac2, showed no effects. Data shown are mean ± s.d. ($n = 3$), expressed as relative cell number compared to control (no chemical treatment). On the *y* axis, 1 = 0.3% Ins+ cells. (**b**) Total ES cell cultures were assayed by immunohistochemistry. Ins staining (yellow) completely overlapped with staining (red) of Pdx1, Nkx6.1 and C-peptide for *in vitro* differentiated ES cells treated on days 11–17 with TBZ and dBu-cAMP. Blue shows DAPI staining. Scale bars, 100 μm. Lower panels are enlarged pictures of the boxes in the top panels. $^*P < 0.05$ and $^{**}P < 0.01$ (two-tailed paired Student's *t*-test).

© 2014 Nature America, Inc. All rights reserved.

pancreatic bud explant culture (**Fig. 3c–g**). We observed a slight decrease in *Amy2b*-expressing exocrine cells but no effects on *Krt19*-expressing duct cells. These results therefore suggested that VMAT2-mediated inhibition of the progress from Pdx1+ pancreatic progenitors to Ngn3+ endocrine progenitors exists in both normal pancreatic endocrine development (**Fig. 3c–g**) and ES cell differentiation (**Fig. 3b**).

The combinatory effects of TBZ and dBu-cAMP addition

Dopamine, histamine and serotonin are considered to function through binding to their receptors. All dopamine, histamine and serotonin receptors are G protein–coupled receptors[22]. In our screen, dibutyryl adenosine 3′,5′-cAMP (dBu-CAMP), a cell-permeable cAMP analog, was identified as a compound to promote β-cell differentiation. We examined the effects of dBu-cAMP and its synergy with TBZ. TBZ or dBu-cAMP alone increased the number of Ins+ cells or the amount of *Ins1* transcript, respectively. Simultaneous addition of TBZ and dBu-cAMP caused an approximately 300-fold increase in *Ins1* transcript, which is approximately 30-fold or 15-fold the effect of single addition of TBZ or dBu-cAMP, respectively (**Fig. 4a**).

In the adult islets, cAMP is known to regulate the potentiation of insulin secretion by a protein kinase A (PKA)-dependent mechanism and a PKA-independent mechanism that involves the cAMP-binding protein Epac2 (ref. 23). As dBu-cAMP activates both pathways[24,25], we then tested a cell-permeable analog, 8CPT-cAMP, that specifically activates Epac2 but not PKA[26]. Ins+ cell number or *Ins1* gene expression did not increase with application of 8CPT-cAMP, and neither showed an additive effect after treatment with 8CPT-cAMP and TBZ. The results suggested that the potentiation of β-cell differentiation by the dBu-cAMP signaling pathway is not mediated through activation of Epac2 but possibly through PKA (**Fig. 4a**).

We then analyzed the differentiated ES cell–derived β cells generated by TBZ and dBu-cAMP treatment by immunocytochemistry. The Ins+ cells expressed Pdx1 and Nkx6.1, which are mature β cell markers. Almost all of the Pdx1+ cells were Ins+. Almost all Ins+ staining overlapped with C-peptide+ staining (**Fig. 4b**). Ins+ cells expressed Nkx2.2, Nkx6.1 and MafA (**Supplementary Fig. 6a**). We also observed *Dolichos biflorus* agglutinin (DBA)+ pancreatic duct cells but not amylase+ exocrine cells in the ES cell culture (**Supplementary Fig. 6b**). There were no qualitative differences in the expression of the above markers among cells treated with both TBZ and dBu-cAMP or each alone (**Supplementary Fig. 6a,b**). We examined whether the Ins+ cells also expressed other endocrine hormones. Although some Ins-single-positive cells, which do not express other endocrine hormones, exist (approximately 10%) in the culture, over 90% of the Ins+ cells were polyhormonal cells, in which glucagon, somatostatin and/or pancreatic polypeptide were also expressed with insulin (**Supplementary Fig. 6**).

As almost all of the Pdx1+ cells derived from ES cells treated with TBZ or dBu-cAMP expressed insulin at the late stage (day 17), which corresponded to the second phase of Pdx1 expression, where Ins is also coexpressed. (**Fig. 1a**), we purified ES cell–derived *Pdx1*-GFP+ cells by flow cytometry (**Fig. 5a,b**) to analyze the β cells with respect to insulin content, GSIS and mRNA expression (**Fig. 5c–e**). *Pdx1*-GFP+ β cells comprised 10.2% of the total cells recovered (**Fig. 5b**). TBZ alone increased C-peptide content to 10 μg per mg, which is approximately 60% of that in adult islets (**Fig. 5c**). However, TBZ did not promote differentiation into cells capable of GSIS (**Fig. 5d**). Isolated *Pdx1*-GFP+ cells treated with dBu-cAMP alone increased GSIS to 170 ng per mg protein per h, which is 42% of that in mature islets (**Fig. 5d**). However, in contrast to TBZ, dBu-cAMP did not increase C-peptide content on a per-protein level (**Fig. 5d**).

The recovery of C-peptide contents from total ES cell–derived cells treated with TBZ, dBu-cAMP or both compounds is summarized in **Supplementary Figure 7a**. ES cell–derived β cells with a C-peptide content equivalent of approximately 100 islets could be obtained from one 96-well plate. The C-peptide contents increased by approximately 5.7-fold or 2.7-fold through treatment with TBZ or dBu-cAMP alone, respectively, and to 8.1-fold through treatment with both compounds (on a per μg DNA basis). This result is consistent with the above result that TBZ and dBu-cAMP additively increased Ins+ cell number.

We also examined the time-dependent effects of the chemicals on GSIS. TBZ alone did not alter GSIS, but dBu-cAMP alone potentiated ES differentiation into Ins+ cells, showing the ability for GSIS from day 15 (**Supplementary Fig. 7b**). To further confirm that the effect of dBu-cAMP occurs through potentiation of differentiation into Ins+ cells, we treated ES cells with dBu-cAMP in different time windows, that is, from day 11 to day 15 or from day 11 to day 17, and then assayed for GSIS on day 17. Treatment with dBu-cAMP for a longer period (day 11 to day 17) significantly ($P < 0.01$) enhanced GSIS compared to those treated from day 11 to day 15 (**Supplementary Fig. 8**). Treatment with dBu-cAMP during the secretion assay significantly ($P < 0.01$) increased GSIS. Therefore, dBu-cAMP treatment potentiated differentiation into matured β cells and enhanced GSIS ability. The results

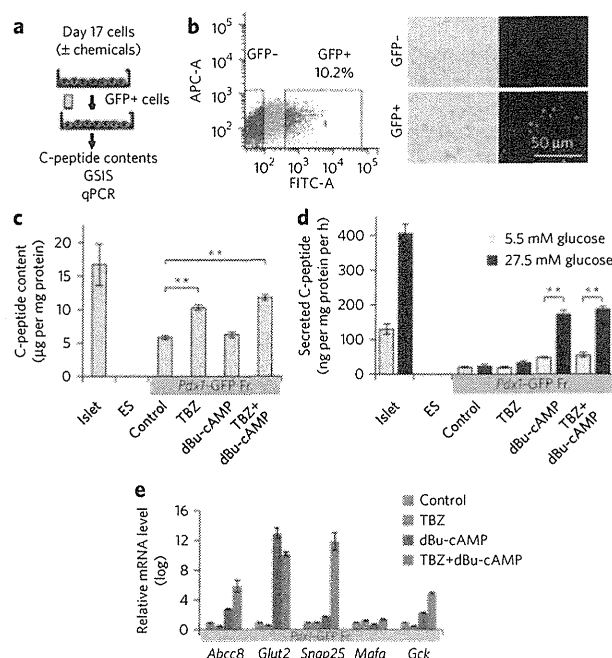

Figure 5 | Characterization of the purified ES cell–derived Ins+ and Pdx-GFP+ cells. TBZ and dBu-cAMP additively potentiated differentiation and maturation of ES cells into β cells with GSIS ability. (**a–e**) Differentiated β cells were purified by flow cytometry. Experimental procedures (**a**) and flow cytometry results (**b**) are shown. Cells were tested for their C-peptide contents (**c**), GSIS (**d**) and quantitative PCR (qPCR) (**e**). In **b**, *Pdx1*-GFP+ cells (10.2% of total cells) were purified by flow cytometry on the basis of GFP intensity. Scale bar, 50 μm. In **c** and **d**, treatment with TBZ alone increased C-peptide content, and treatment with dBu-cAMP alone evoked GSIS, as measured by C-peptide contents or secreted C-peptide with significant differences (two-tailed paired Student's *t*-test) $^{**}P < 0.01$. (**e**) Quantitative PCR was performed to quantify the expression of *Abcc8*, *Glut2*, *Snap25*, *Mafa* and *Gck*. In **c–e**, GFP+ cells from differentiated ES cells were used, to which DMSO (no chemical treatment), TBZ or dBu-cAMP or both (TBZ + dBu-cAMP) were added. In **c**, $n = 4$, and in **d** and **e**, $n = 3$.

© 2014 Nature America, Inc. All rights reserved.

showing that dBu-cAMP potentiated GSIS suggested that the enhancement of differentiation may be mediated by insulin. The effect of insulin was then examined by manipulating the insulin concentration in medium III (**Fig. 1a**), which contained 10 μM insulin in all of the experiments reported so far. Insulin potentiated the differentiation at 16 nM, and its effect declined with increasing insulin concentrations (**Supplementary Fig. 9**). Therefore, TBZ plus dBu-cAMP enhanced insulin secretion at low levels, which in turn accelerated the expression of *Ins1* and further drove β-cell differentiation.

Real-time PCR analyses revealed that dBu-cAMP administration alone increased the expression of genes implicated in GSIS: *Abcc8*, which encodes the regulatory sulfonylurea receptor SUR of the ATP-sensitive potassium channel, and the glucose transporter–encoding genes *Slc2a2* (also known as *Glut2*) and *Gck* (**Fig. 5e**). Double treatment with TBZ and dBu-cAMP upregulated expression of *Abcc8* and *Gck* by $\sim 1 \times 10^5$–fold and upregulated expression of *Glut2* and *Snap25*, which encodes a component involved in the regulation of vesicular release, by $\sim 1 \times 10^{10}$–fold compared to expression in the control (**Fig. 5e**).

Taken together, these results indicated that TBZ treatment increased insulin content and dBu-cAMP increased GSIS of the ES cell–derived cells. Simultaneous treatment with TBZ and dBu-cAMP enabled the ES cell–derived β cells to produce Ins and secrete Ins *in vitro* in a glucose-sensitive manner at levels comparable to that of adult islets.

The transplanted cells reversed hyperglycemia in mice

To examine their *in vivo* function, we transplanted ES cell–derived β cells into AKITA mice with immunodeficiency ($Rag1^{-/-}$ $Ins2^{Akita/+}$)[27]. The AKITA mouse is a model that inherits diabetes in a dominant manner owing to a missense mutation in *Ins2*. Consistent with our previous report[28], all male heterogeneous AKITA mice gradually developed hyperglycemia after they reached 6 weeks of age (**Supplementary Fig. 10a**). We harvested 4×10^6 or 1×10^7 ES cell–derived cells (treated with both TBZ and dBu-cAMP) on day 17 and grafted the cells under the kidney capsule in each experimental mouse. The experimental mice showed a reversal of hyperglycemia for more than 6 weeks, with larger grafts showing increasing effects (**Supplementary Fig. 10a**), whereas no change in blood glucose was observed in control untransplanted AKITA mice.

We then transplanted 1×10^7 ES cell–derived cells, which were treated with no chemical, TBZ or dBu-cAMP alone or with both TBZ and dBu-cAMP, into the kidney capsule of the AKITA mice. Mice engrafted with cells that were not treated with growth factors served as negative controls. Mice transplanted with cells treated with TBZ plus dBu-cAMP or dBu-cAMP alone partially recovered from hyperglycemia and showed lowered fasting blood glucose as early as 2 weeks after engraftment (**Fig. 6a**). Mice engrafted with cells treated with both TBZ and dBu-cAMP completely recovered from glucose intolerance, whereas those engrafted with cells treated with dBu-cAMP alone did not (**Fig. 6a–c**). In both cases, the engrafted mice showed even higher levels of plasma C-peptide compared to that in the control wild-type BL6 mice (**Supplementary Fig. 10b**). The AKITA mice are reported to be insulin resistant[29]. The above results might reflect the insulin resistance of the recipient AKITA mice. In contrast, mice engrafted with cells treated with TBZ alone responded to glucose administration and increased plasma C-peptide levels more rapidly compared to those engrafted with control cells (no chemical treatment) (**Supplementary Fig. 10b**), which agreed with their partial reversal of glucose tolerance (**Fig. 6b**) and fasting blood glucose (**Fig. 6a**).

Grafts without noticeable tumor formation were recovered from the experimental mice and were found to express insulin (**Supplementary Fig. 10c**). No insulin-positive cells coexpressed glucagon, pancreas polypeptide or somatostatin. We confirmed that the β-cell mass in the recipient AKITA pancreas did not increase after transplantation, showing an altered allocation of glucagon+ cells at the center of the islets, in contrast to their peripheral localization in the control wild-type mice (**Supplementary Fig. 10d**). Taken together, we concluded that the reversal of hyperglycemia and restoration of glucose tolerance was due to the transplanted ES cell–derived cells.

These results demonstrate that treatment of both TBZ and dBu-cAMP potentiated differentiation of ES cells into cells, with a high level of C-peptide contents and GSIS ability, and transplantation of these cells reversed hyperglycemia in AKITA diabetic mice.

DISCUSSION

Although the function of VMAT2 in the pancreas is largely unknown, VMAT2 is known to take up monoamines such as dopamine, histamine and serotonin into secretory granules of neurons and exert both autocrine and paracrine functions in the nervous system. VMAT2 is described to be expressed in human β cells. However, there has been some controversy in the literature about its presence in β cells of rodents[30]. Here, the target cells of the VMAT2 inhibitors are differentiating pancreatic progenitor cells. We revealed a new role of VMAT2 and monoamine-dependent suppression of differentiation from the pancreatic progenitor cells.

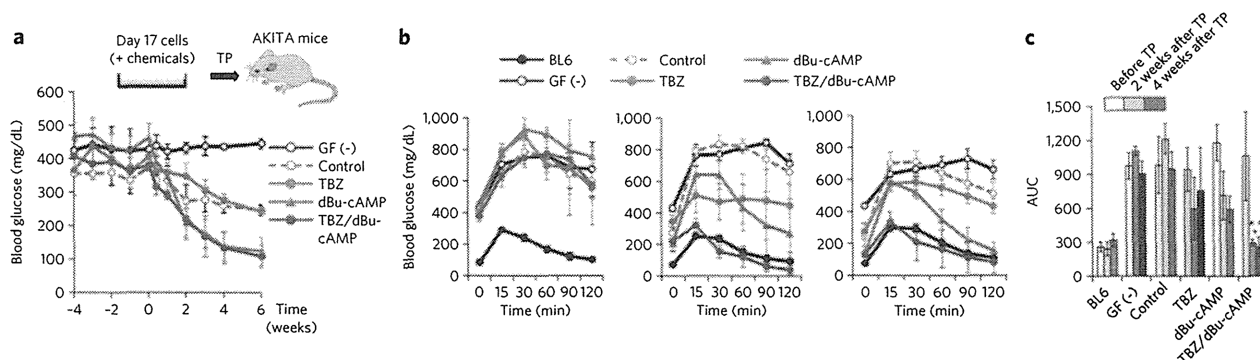

Figure 6 | Transplanted cells reversed hyperglycemia and glucose tolerance. Transplantation assays showed that the induced β cells normalized fasting blood glucose levels and glucose tolerance in the AKITA diabetic mice. (**a**) Top, experimental procedure. *In vitro* differentiated β cells, treated with TBZ and dBu-cAMP, were harvested on day 17 and transplanted into hyperglycemic AKITA mice. Bottom, fasting blood glucose levels (mg/dL) of mice transplanted with ES-derived β cells were measured before and after engraftment. X axis shows weeks after transplantation. (**b**) AKITA mice were analyzed for IPGTT before engraftment (left), 2 weeks (middle) or 4 weeks (right) after engraftment, and time courses of blood glucose levels (mg/dL) after challenge with glucose are shown. X axis shows minutes after glucose challenges. (**c**) Area under curve (AUC) of IPGTT curves shown in **b**. Light color bars, before engraftment; darker color bars, 2 weeks after engraftment; darkest color bars, 4 weeks after engraftment. In **a** and **b**, blue circles represent treatment with TBZ, green circles represent treatment with dBu-cAMP, purple circles represent treatment with TBZ and dBu-cAMP, broken lines with open circles represent no chemical treatment at 1×10^7, and black lines with open circles represent cells with no growth factor treatment (negative controls). In **a**–**c**, the significant differences between treatment and control were $^*P < 0.05$ or $^{**}P < 0.01$ (two-tailed unpaired Student's *t*-test) and are indicated above error bars, which show s.d.

© 2014 Nature America, Inc. All rights reserved.

Dopamine, histamine and serotonin are synthesized and stored in the endocrine pancreas during pregnancy[31] and in adult β cells[19]. In the adult, there are several lines of evidence supporting that dopamine and histamine negatively regulate insulin content, glucose tolerance[32–34] and GSIS[35–37]. In contrast, serotonin is reported to drive β-cell replication and regulate glucose tolerance in pregnant mice. However, the role of monoamines during embryonic development remains largely unknown.

Among the monoamines, dopamine is produced at a highest level in ES cell–derived cells and during embryonic stages. Consistent with this, dopamine synthesizing enzyme (encoded by *Th*), was expressed in the ES-derived cells at a level comparable to that in the embryonic pancreas. In spite of the differences in their cellular contents, inhibition of all three synthesizing enzymes showed similar effects to enhance β-cell differentiation, indicating that all of these monoamines take part in this process. It was puzzling that application of these monoamines dose-dependently suppressed β cell differentiation with similar EC_{50} values, although their EC_{50} against their specific receptors are very different[38–40]. We hypothesize that this is due to the fact that monoamine is taken up into the storage vesicles and their subsequent release is required for their action and that other components co-released from the vesicle might be required to convey their function[41].

Our results indicated that monoamines controlled by VMAT2 serve as a brake for differentiation of Pdx1+ pancreatic progenitors into Ngn3+ endocrine precursors and subsequently into Ins+ cells. Once this brake is released, the Pdx1+ cells are induced to differentiate into Ngn3+ cells, which quickly turn into Ins+ cells. TBZ acted during a short time window to increase Ngn3+ cells, suggesting that this brake functions transiently. However, whether there are specific roles for each of the monoamines remains an open question.

In the adult β cells, GLP1 and GIP are well known to activate $G\alpha_s$-coupled receptors and potentiate GSIS by activating cAMP signaling and modulating K_{ATP} channel activity. It is reported that cAMP signaling induces glucose responsiveness through both PKA and Epac2 dependent pathway[23]. PKA is reported to modulate VMAT2 by regulating its trafficking[42]. It is possible that cAMP activates β-cell differentiation through modulating VMAT2. It remains unknown whether GLP1, GIP or other unknown ligands function to promote the maturation of β cells to initiate GSIS during embryonic development. This would agree with the observation that pancreas-specific $G\alpha_s$-deficient mice demonstrated reduced β-cell mass and defects in glucose response[43].

Most of the ES cell–derived insulin+ cells were polyhormonal cells, coexpressing other endocrine hormones. Maturation rapidly occurred *in vivo*. They rapidly turned into insulin-single positive cells after they were grafted under kidney capsules. Intrapenitoneal glucose trelant test (IPGTT) results revealed that cells doubly treated with TBZ and dBu-cAMP matured into cells capable of GSIS and restored glucose tolerance as early as 2 weeks after engraftment. Cells treated with TBZ alone or with no chemicals also matured *in vivo* and became potent for GSIS within 2 weeks. In mouse pancreatic development, Ins+ glucagon+ cells appear early in 'first transition', and they do not contribute to the generation of mature β cells[44]. These cells do not express mature endocrine markers[45]. By contrast, Ins+ glucagon+ transitional cells exist transiently during the conversion of α cells into β cells[46,47]. The polyhormonal cells observed in the present study expressed mature endocrine markers. Therefore, the ES cell–derived polyhormonal cells here might have characteristics close to the transitional cells that appear during cell fate conversion rather than those that exist during early mouse embryonic development. Although the exact mechanism of how ES cells mature under *in vivo* environment remains unknown, it is reported that dynamic chromatin remodeling occurs in human ES cells after they are engrafted *in vivo*[48]. Previous studies have shown that human ES cell–derived insulin-expressing cells, which are polyhormonal, differentiate into α cells, instead of β cells, after transplantation[49]. The discrepancies might be due to the differences in the underlying mechanism between the mouse and human ES cells or due to the differences between the culture protocols. However, it is technically difficult for us to perform further long-term analyses, such as transplantation or re-culture of the mouse ES cell–derived Pdx1/GFP+ cells, owing to a significant ($P < 0.01$) loss of cell viability after sorting at this late stage of differentiation. Taken together, although we cannot completely rule out other possibilities, our results suggested that the transplanted insulin-expressing cells reversed hyperglycemia in AKITA mice.

The graft experiments showed that transplanting 4×10^6 or 1×10^7 ES cell–derived cells, with their C-peptide contents equivalent to 40 or 100 islets, respectively, is enough to reverse hyperglycemia in AKITA diabetic mice. This is lower than the previously reported observation that it is necessary to transplant 150–200 islets to reverse hyperglycemia[50]. Our results suggested that these ES cell–derived cells rapidly underwent further differentiation *in vivo* and increased their C-peptide contents or GSIS ability so that a lower number of ES cell–derived cells was enough for the reversal of hyperglycemia.

The ES cell–derived cells showed no signs of tumor formation. This might due to the high differentiation efficiency into the definitive endoderm. Moreover, the long differentiation period might also result in a low population of undifferentiated cells remaining in culture.

In conclusion, results of the present study demonstrated a previously unknown function of VMAT2 in controlling differentiation into pancreatic endocrine precursors. VMAT2 inhibition and dBu-cAMP addition synergized and further increased *Ins1* transcripts and are sufficient to promote differentiation of ES cells into functional β cells capable of reversing hyperglycemia in diabetic mice. Future studies would be required to analyze the role of VMAT2 during human induced pluripotent stem cell cell differentiation to apply this protocol for future cell replacement therapy.

Received 15 December 2012; accepted 15 October 2013; published online 15 December 2013

METHODS

Methods and any associated references are available in the online version of the paper.

© 2014 Nature America, Inc. All rights reserved.

References

1. Jonsson, J., Carlsson, L., Edlund, T. & Edlund, H. Insulin-promoter-factor 1 is required for pancreas development in mice. *Nature* **371**, 606–609 (1994).
2. Gu, G., Dubauskaite, J. & Melton, D.A. Direct evidence for the pancreatic lineage: NGN3+ cells are islet progenitors and are distinct from duct progenitors. *Development* **129**, 2447–2457 (2002).
3. Gradwohl, G., Dierich, A., LeMeur, M. & Guillemot, F. *neurogenin3* is required for the development of the four endocrine cell lineages of the pancreas. *Proc. Natl. Acad. Sci. USA* **97**, 1607–1611 (2000).
4. Puri, S. & Hebrok, M. Cellular plasticity within the pancreas—lessons learned from development. *Dev. Cell* **18**, 342–356 (2010).
5. D'Amour, K.A. *et al.* Efficient differentiation of human embryonic stem cells to definitive endoderm. *Nat. Biotechnol.* **23**, 1534–1541 (2005).
6. Skoudy, A. *et al.* Transforming growth factor (TGF)β, fibroblast growth factor (FGF) and retinoid signalling pathways promote pancreatic exocrine gene expression in mouse embryonic stem cells. *Biochem. J.* **379**, 749–756 (2004).
7. D'Amour, K.A. *et al.* Production of pancreatic hormone-expressing endocrine cells from human embryonic stem cells. *Nat. Biotechnol.* **24**, 1392–1401 (2006).
8. Borowiak, M. *et al.* Small molecules efficiently direct endodermal differentiation of mouse and human embryonic stem cells. *Cell Stem Cell* **4**, 348–358 (2009).
9. Chen, S. *et al.* A small molecule that directs differentiation of human ESCs into the pancreatic lineage. *Nat. Chem. Biol.* **5**, 258–265 (2009).
10. Shiraki, N. *et al.* Guided differentiation of embryonic stem cells into Pdx1-expressing regional-specific definitive endoderm. *Stem Cells* **26**, 874–885 (2008).
11. Higuchi, Y. *et al.* Synthesized basement membranes direct the differentiation of mouse embryonic stem cells into pancreatic lineages. *J. Cell Sci.* **123**, 2733–2742 (2010).
12. Wang, Y.M. *et al.* Knockout of the vesicular monoamine transporter 2 gene results in neonatal death and supersensitivity to cocaine and amphetamine. *Neuron* **19**, 1285–1296 (1997).
13. Pothos, E.N. *et al.* Synaptic vesicle transporter expression regulates vesicle phenotype and quantal size. *J. Neurosci.* **20**, 7297–7306 (2000).
14. Vergo, S., Johansen, J.L., Leist, M. & Lotharius, J. Vesicular monoamine transporter 2 regulates the sensitivity of rat dopaminergic neurons to disturbed cytosolic dopamine levels. *Brain Res.* **1185**, 18–32 (2007).
15. Eiden, L.E. & Weihe, E. VMAT2: a dynamic regulator of brain monoaminergic neuronal function interacting with drugs of abuse. *Ann. NY Acad. Sci.* **1216**, 86–98 (2011).
16. Erickson, J.D., Schafer, M.K., Bonner, T.I., Eiden, L.E. & Weihe, E. Distinct pharmacological properties and distribution in neurons and endocrine cells of two isoforms of the human vesicular monoamine transporter. *Proc. Natl. Acad. Sci. USA* **93**, 5166–5171 (1996).
17. Anlauf, M. *et al.* Expression of the two isoforms of the vesicular monoamine transporter (VMAT1 and VMAT2) in the endocrine pancreas and pancreatic endocrine tumors. *J. Histochem. Cytochem.* **51**, 1027–1040 (2003).
18. Simpson, N.R. *et al.* Visualizing pancreatic β-cell mass with [^{11}C]DTBZ. *Nucl. Med. Biol.* **33**, 855–864 (2006).
19. Saisho, Y. *et al.* Relationship between pancreatic vesicular monoamine transporter 2 (VMAT2) and insulin expression in human pancreas. *J. Mol. Histol.* **39**, 543–551 (2008).
20. Grimsby, J., Chen, K., Wang, L.J., Lan, N.C. & Shih, J.C. Human monoamine oxidase A and B genes exhibit identical exon-intron organization. *Proc. Natl. Acad. Sci. USA* **88**, 3637–3641 (1991).
21. Gu, G. *et al.* Global expression analysis of gene regulatory pathways during endocrine pancreatic development. *Development* **131**, 165–179 (2004).
22. Kroeze, W.K., Sheffler, D.J. & Roth, B.L. G-protein-coupled receptors at a glance. *J. Cell Sci.* **116**, 4867–4869 (2003).
23. Seino, S., Shibasaki, T. & Minami, K. Dynamics of insulin secretion and the clinical implications for obesity and diabetes. *J. Clin. Invest.* **121**, 2118–2125 (2011).
24. Lo, K.W., Kan, H.M., Ashe, K.M. & Laurencin, C.T. The small molecule PKA-specific cyclic AMP analogue as an inducer of osteoblast-like cells differentiation and mineralization. *J. Tissue Eng. Regen. Med.* **6**, 40–48 (2012).
25. Mei, F.C. *et al.* Differential signaling of cyclic AMP: opposing effects of exchange protein directly activated by cyclic AMP and cAMP-dependent protein kinase on protein kinase B activation. *J. Biol. Chem.* **277**, 11497–11504 (2002).
26. Kelley, G.G. *et al.* Glucose-dependent potentiation of mouse islet insulin secretion by Epac activator 8-pCPT-2′-*O*-Me-cAMP-AM. *Islets* **1**, 260–265 (2009).
27. Wang, J. *et al.* A mutation in the insulin 2 gene induces diabetes with severe pancreatic β-cell dysfunction in the *Mody* mouse. *J. Clin. Invest.* **103**, 27–37 (1999).
28. Mochida, T. *et al.* Time-dependent changes in the plasma amino acid concentration in diabetes mellitus. *Mol. Genet. Metab.* **103**, 406–409 (2011).
29. Hong, E.G. *et al.* Nonobese, insulin-deficient Ins2Akita mice develop type 2 diabetes phenotypes including insulin resistance and cardiac remodeling. *Am. J. Physiol. Endocrinol. Metab.* **293**, E1687–E1696 (2007).
30. Schäfer, M.K. *et al.* Species-specific vesicular monoamine transporter 2 (VMAT2) expression in mammalian pancreatic β cells: implications for optimising radioligand-based human β cell mass (BCM) imaging in animal models. *Diabetologia* **56**, 1047–1056 (2013).
31. Harris, P.E. *et al.* VMAT2 gene expression and function as it applies to imaging β-cell mass. *J. Mol. Med.* **86**, 5–16 (2008).
32. Fülöp, A.K. *et al.* Hyperleptinemia, visceral adiposity, and decreased glucose tolerance in mice with a targeted disruption of the histidine decarboxylase gene. *Endocrinology* **144**, 4306–4314 (2003).
33. Buchanan, T.A. & Xiang, A.H. Gestational diabetes mellitus. *J. Clin. Invest.* **115**, 485–491 (2005).
34. Kim, H. *et al.* Serotonin regulates pancreatic β cell mass during pregnancy. *Nat. Med.* **16**, 804–808 (2010).
35. Rubí, B. *et al.* Dopamine D2-like receptors are expressed in pancreatic β cells and mediate inhibition of insulin secretion. *J. Biol. Chem.* **280**, 36824–36832 (2005).
36. Ericson, L.E., Hakanson, R. & Lundquist, I. Accumulation of dopamine in mouse pancreatic B-cells following injection of l-DOPA. Localization to secretory granules and inhibition of insulin secretion. *Diabetologia* **13**, 117–124 (1977).
37. Zern, R.T., Bird, J.L. & Feldman, J.M. Effect of increased pancreatic islet norepinephrine, dopamine and serotonin concentration on insulin secretion in the golden hamster. *Diabetologia* **18**, 341–346 (1980).
38. Seeman, P. *et al.* The dopaminergic stabilizer ASP2314/ACR16 selectively interacts with $D2^{High}$ receptors. *Synapse* **63**, 930–934 (2009).
39. Braden, M.R., Parrish, J.C., Naylor, J.C. & Nichols, D.E. Molecular interaction of serotonin 5-HT2A receptor residues $Phe339^{(6.51)}$ and $Phe340^{(6.52)}$ with superpotent *N*-benzyl phenethylamine agonists. *Mol. Pharmacol.* **70**, 1956–1964 (2006).
40. Peakman, M.C. & Hill, S.J. Endogenous expression of histamine H1 receptors functionally coupled to phosphoinositide hydrolysis in C6 glioma cells: regulation by cyclic AMP. *Br. J. Pharmacol.* **113**, 1554–1560 (1994).
41. El Mestikawy, S., Wallen-Mackenzie, A., Fortin, G.M., Descarries, L. & Trudeau, L.E. From glutamate co-release to vesicular synergy: vesicular glutamate transporters. *Nat. Rev. Neurosci.* **12**, 204–216 (2011).
42. Yao, J., Erickson, J.D. & Hersh, L.B. Protein kinase A affects trafficking of the vesicular monoamine transporters in PC12 cells. *Traffic* **5**, 1006–1016 (2004).
43. Xie, T., Chen, M. & Weinstein, L.S. Pancreas-specific Gs_{α} deficiency has divergent effects on pancreatic α- and β-cell proliferation. *J. Endocrinol.* **206**, 261–269 (2010).

44. Herrera, P.L. Adult insulin- and glucagon-producing cells differentiate from two independent cell lineages. *Development* **127**, 2317–2322 (2000).
45. Murtaugh, L.C. Pancreas and β-cell development: from the actual to the possible. *Development* **134**, 427–438 (2007).
46. Collombat, P. *et al.* The ectopic expression of Pax4 in the mouse pancreas converts progenitor cells into alpha and subsequently β cells. *Cell* **138**, 449–462 (2009).
47. Thorel, F. *et al.* Conversion of adult pancreatic α-cells to β-cells after extreme β-cell loss. *Nature* **464**, 1149–1154 (2010).
48. Xie, R. *et al.* Dynamic chromatin remodeling mediated by polycomb proteins orchestrates pancreatic differentiation of human embryonic stem cells. *Cell Stem Cell* **12**, 224–237 (2013).
49. Kelly, O.G. *et al.* Cell-surface markers for the isolation of pancreatic cell types derived from human embryonic stem cells. *Nat. Biotechnol.* **29**, 750–756 (2011).
50. Yasunami, Y. *et al.* Vα14 NK T cell-triggered IFN-γ production by Gr-1+CD11b+ cells mediates early graft loss of syngeneic transplanted islets. *J. Exp. Med.* **202**, 913–918 (2005).

Acknowledgments

We thank members of the Gene Technology Center and Center for Animal Resources and Development at Kumamoto University for technical assistance. This work was supported by the Funding Program for Next Generation World-Leading Researchers (to S.K. (no. LS099) and M.U.); the Japan Society for the Promotion of Science, the Realization of Regenerative Medicine (to S.K. and M.U.); the Program for Leading Graduate Schools 'HIGO' (awarded to S.K.); Grants-in-Aid from the Ministry of Education, Culture, Sports, Science and Technology (MEXT), Japan (no. 21390280 to S.K. and no. 22790653 to D. Sakano); and the Collaborative Research Program of Institute for Chemical Research, Kyoto University (grant no. 2010-44). The iCeMS is supported by World Premier International Research Center Initiative, MEXT, Japan.

Author contributions

D. Sakano performed chemical screening, cellular and biochemical analyses; D. Sakano, N.S. and K.U. established the ES cell differentiation system; D. Sakano, K. Kikawa, M.K. and T.Y. performed transplantation assays; K.A. established the ES cell line; S.M., F.E. and N.N. helped maintain AKITA mice; D.M. and M.U. provided and analyzed the chemical library; O.A. and D. Stainier provided chemicals; K. Kume and S.K. provided technical advices, S.K. designed the experiments and wrote the paper. All of the authors discussed the results and commented on the manuscript.

Competing financial interests

The authors declare no competing financial interests.

Additional information

Supplementary information and chemical compound information is available in the online version of the paper. Reprints and permissions information is available online at http://www.nature.com/reprints/index.html. Correspondence and requests for materials should be addressed to S. Kume.

© 2014 Nature America, Inc. All rights reserved.

ONLINE METHODS

Ethics statement. This animal work is approved by the Institutional Review Board for Animal Care and Use of Kumamoto University. All animal procedures were conducted according to Kumamoto University guideline.

ES cell lines. The SK7 ES cell line[10] was established from a transgenic mouse line bearing the *Pdx1*-GFP gene. NGP9 ES cells were established by culturing blastocysts obtained from transgenic mice heterozygous for the *Ngn3*-GFP gene[21]. SK7 and NGP9 cells were maintained on MEF feeder cells in Dulbecco's modified Eagle's medium (DMEM; Invitrogen, Carlsbad, CA) supplemented with leukemia inhibitory factor (LIF), 10% FBS, nonessential amino acids (NEAA), L-glutamine (L-Gln), penicillin and streptomycin (PS) and β-mercaptoethanol (β-ME)[10].

Differentiation of ES cells into pancreatic β cells. For differentiation studies, ES cells were plated at 5,000 cells per well, in Corning 96-well plates with Ultra-Web Synthetic Polyamine Surface (no. 3873XX1, Corning Coster, Cambridge, MS). The cells were cultured for 7 d in Medium I: Dulbecco's Modified Eagle Medium (DMEM: Invitrogen, Glasgow, UK) containing 4,500 mg/L glucose and supplemented with 100 μM nonessential amino acids (NEAA), 2 mM L-glutamine (L-Gln; Nacalai tesque, Japan), 1 mM sodium pyruvate (Invitrogen), 50 units/mL penicillin, 50 μg/mL streptomycin (PS; Nacalai tesque), 100 μM β-mercaptoethanol (β-ME; Sigma-Aldrich), ITS (10 μg/mL insulin (Sigma-Aldrich), 5.5 μg/mL transferrin (Sigma-Aldrich) and 6.7 pg/mL selenium (Sigma-Aldrich)), 0.25% Albmax (Invitrogen), 10 ng/ml recombinant human Activin-A (R&D Systems, Minneapolis, MN) and 5 ng/mL recombinant human bFGF (Peprotech). On days 7–11, the cells were cultured in Medium II: RPMI 1640 medium (Invitrogen) containing 2,000 mg/L glucose (Sigma, St. Louis, MO), 1 μM retinoic acid (Sigma-Aldrich), 50 ng/mL human recombinant fibroblast growth factor-10 (human recombinant FGF10, Peprotech, Rocky Hill, NJ), 2% B-27 Supplement (Invitrogen) and 0.25 μM of the Shh signaling antagonist 3-keto-*N*-(aminoethyl-aminocaproyl-dihydrocinnamoyl) cyclopamine (KAAD-cyclopamin, Calbiochem, San Diego, CA). Finally, on days 11–17, cells were cultured in Medium III: DMEM containing 1,000 mg/L glucose supplemented with NEAA, L-Gln, PS, β-ME, ITS, 0.25% Albmax (Invitrogen), 10 nM glucagon-like peptide 1 (GLP-1, Sigma-Aldrich) and 10 mM nicotinamide (NA, Sigma-Aldrich). The medium was replaced every 2 d.

© 2014 Nature America, Inc. All rights reserved.
npg

Screening of small molecules and quantitative analysis of imaging. Small molecules from the bioactive, pharmacologically defined Prestwick Chemical Library were screened for pro-differentiation factors. Compounds were dissolved in DMSO (Sigma-Aldrich) and added at 1:100 on day 11, with changes on days 13 and 15. Cells were assayed by immunostaining with mouse anti-insulin (Sigma-Aldrich; I2018; 1:1,000) on day 17. Fluorescent images were quantified by counting pixel numbers representing the number of positive cells, using a ImageXpress Micro scanning system and MetaXpress cellular image analysis software (Molecular Devices, Japan). Data were normalized as fold change relative to DMSO controls. Hit compounds were defined as causing a twofold or higher increase in insulin-positive β cells. Candidate compounds were tested for dose dependency and reproducibility. The screening information is summarized in **Supplementary Table 1**.

Chemicals. Reserpine was purchased from Calbiochem Novabiochem Novagen, TBZ was purchased from Tocris Bioscience, and dibutyryl-cAMP (dBu-cAMP) was purchased from BIOMOL International.

Pargyline was purchased from Cayman Chemicals. The compounds were dissolved in DMSO (final concentration = 1.0%) and added on days 11, 13 and 15. After initial screening, the following concentrations were used: 0.63 μM reserpine, 1.25 μM TBZ, 0.1 μM dopamine (LKT Labs, Inc.), 0.6 μM dBu-cAMP, 1.0 μM pargyline, 1.3 μM α-methyltyrosine (α-MT, Sigma-Aldrich), 0.6 μM L-3,4-dihydroxyphenylalanine (L-DOPA, Toronto Research Chemicals Inc,), 1.3 μM α-fluoromethyl- histidine (α-FMH, Toronto Research Chemicals Inc,), 1.3 μM 5-hydroxy tryptophan (5HTP, Sigma-Aldrich) and 0.6 μM carbachol (Sigma-Aldrich), unless otherwise specified.

Chemical characterization. To confirm the purity of reserpine, TBZ and dBu-cAMP, we checked their HPLC, LC-MS (ESI), and ^{1}H-NMR profiles. The results showed that the reagents we used had high purity (>90%) (**Supplementary Figs. 11–13**). HPLC analysis was performed with a Shimadzu LC-2010C equipped with reversed-phase HPLC column (GL science, Inertsil ODS-3, 4.6 × 150 mm, flow rate 1.0 mL/min, 0.1% TFA CH_3CN/H_2O, 10–100%). Mass spectra (ESI) were recorded on a Shimadzu LCMS-2010. ^{1}H-NMR spectra were collected on a JEOL JNM-ECP (300 MHz).

Immunocytochemistry. For immunocytochemistry, ES cells were fixed with 4% paraformaldehyde and processed after 13 days in culture (**Fig. 3** and **Supplementary Fig. 5**), 17 d in culture (**Figs. 1, 2** and **4** and **Supplementary Fig. 6**) or 6 weeks after transplantation (**Supplementary Fig. 10**). For examination of target protein expression in single cells, ES cell–derived differentiated cells were dissociated with 0.25% trypsin (Invitrogen), replated for 30 min and then fixed and processed for immunocytochemistry. The following antibodies were used: rabbit anti-MafA (Abcam; ab17976; 1/100,), rabbit anti–C-peptide (Cell Signaling; 4593, 1/100), guinea pig anti-insulin (Dako; A0564; 1/1,000), rabbit anti-pancreatic polypeptide (Dako; A619; 1/100), mouse anti-Nkx2.2 (Developmental Studies Hybridoma Bank, University of Iowa; 74.5A5; 1/100), mouse anti-Nkx6.1 (Developmental Studies Hybridoma Bank, University of Iowa; F64A6B4; 1/100), rabbit anti-GFP (MBL International Corp; 598; 1/1,000), goat anti-Pdx1 (R&D systems; AF2419, 1/100), goat anti-amylase (Santa Cruz Biotechnology; sc-12821; 1/100), goat anti-somatostatin (Santa Cruz Biotechnology; sc-7819; 1/100), mouse anti-glucagon (Sigma-Aldrich; G2654; 1/1,000), biotin-conjugated *D. biflorus* agglutinin (DBA) lectin (Sigma-Aldrich; L6533; 1/500) and mouse anti-insulin (Sigma-Aldrich; I2018; 1/1,000) antibodies were used. Secondary antibodies used were Alexa 488–conjugated goat anti-mouse IgG (A11029; 1/1,000), Alexa 568–conjugated goat anti-guinea pig IgG (A11075; 1/1,000), Alexa 568–conjugated goat anti-mouse IgG (A11031; 1/1,000), Alexa 568–conjugated goat anti-rabbit IgG (A11036; 1/1,000), Alexa 568–conjugated anti-streptabidine antibody (S11223; 1/1,000), or Alexa 633–conjugated donkey anti-goat IgG (A21082; 1/1,000), Alexa 633–conjugated goat anti-mouse IgG (A21053; 1/1,000), Alexa 633–conjugated goat anti-rabbit IgG (A21072; 1/1,000) (all from Invitrogen). Cells were counterstained with DAPI (Roche Diagnotics, Basel, Switzerland).

Gene silencing. In the VMAT2-knockdown assays, cells were transfected with Expression Arrest nonsilencing, control shRNA (Open Biosystems, no. RHS4080), VMAT2 shRNA (Open Biosystems, no. RMM3981-97058457 and no. RMM3981-97058458). The lentiviral vectors were constructed as previously described[11]. SK7 cells were infected with viral supernatants. After 24 h of incubation, the virus-containing medium was replaced with fresh ES maintenance medium. After 24 h of incubation, infected cells were selected using 1.5 μg/mL puromycin (Sigma-Aldrich). The surviving cells were harvested, and clones were selected to establish knockdown and control cell lines.

Measurement of intracellular monoamine levels. Cells were treated with chemicals before harvest (days 11–17). Cells were lysed with lysis buffer containing 0.1% Triton X-100 (Nakarai Tesque, Japan) in 0.1 M PBS (pH7.2, Sigma-Aldrich) with protease inhibitor cocktail. Lysates were assayed for dopamine, histamine, serotonin, adrenaline or noradrenaline with each monoamine-specific ELISA kit (Labor Diagnostika Nord GmbH & Co.; KG Nordhorn Germany).

EdU incorporation. Cells were treated with culture medium containing 20 μM 5-ethynyl-2′-deoxyuridine (EdU) for 48 h before harvest (days 17–19), processed using the Click-iT EdU Alexa Fluor 594 Imaging Kit (Invitrogen) and stained with DAPI and anti-GFP antibodies, rabbit anti-GFP (no. 598; 1:1,000; MBL International Corp., Woburn, MA) and detected with Alexa 488-conjugated goat anti-rabbit IgG (Invitrogen; A-11008; 1:1,000).

Pancreas bud *in vitro* culture. Pancreas buds were dissected from E12.5 embryos of a transgenic mouse line bearing the *Pdx1*- green fluorescent protein (GFP) gene. The tissue was placed onto 12-well Corning Transwell cell culture inserts (Corning Coster, Cambridge, MS). The bottom of the inserts were touched with medium containing M199 with NEAA, L-Gln, PS, β-ME and 10% FBS (FBS, Hyclone).

Flow cytometry. Cells were collected and suspended in 1 × HANKS with 1% FBS. A FACS Aria II flow cytometry cell sorter (Becton Dickinson Immunocytometry Systems, San Jose, CA) was used to purify GFP-positive cells by sorting them against the fluorescence profiles of differentiating cells prepared from wild-type mice. Dead cells were identified using propidium iodide (Sigma-Aldrich).

Quantitative real-time PCR. RNA was extracted from ES cells, mouse tissue or transplanted grafts using the RNeasy minikit (Qiagen, Hilden, Germany) and then treated with DNase I (Qiagen).

Complementary DNA was synthesized from 1 μg of total RNA using Revertra Ace qPCR RT Master Mix (Toyobo).

For real-time PCR analysis, the mRNA expression was quantified with SyberGreen on an ABI 7500 thermal cycler (Applied Biosystems, Foster City, CA). The level of expression of each gene was normalized with that of the β-actin–expressing gene *Actb* . The PCR conditions were as follows: denaturation at 95 °C for 15 s, annealing and extension at 60 °C for 60 s for up to 40 cycles. Each measurement was normalized to *Actb* (mouse) expression for each sample by subtracting the average *Actb* (mouse) expression. C_t values (threshold cycle) from the average Each gene C_t, resulting in C_t Target mRNA levels are expressed as arbitrary units. All of the primers for real-time PCR are listed in **Supplementary Table 2.**

Measurement of glucose-stimulated C-peptide secretion and cellular or plasma C-peptide level by enzyme-linked immunosorbent assay. Differentiating ES cells were preincubated for 0.5 h in low glucose (5.5 mM) DMEM with minimal essential medium and 1% FBS. Cells were washed twice with phosphate-buffered saline then incubated for 2 h in low-glucose (5.5 mM) or high-glucose (27.5 mM) DMEM with 1% FBS. The culture medium was collected, and cells were lysed with a lysis buffer of 0.1% Triton X-100 in PBS with added protease inhibitor cocktail. Insulin secretion into the culture medium and insulin content of the cell lysates were measured using a mouse C-peptide ELISA kit (Shibayagi Co. Ltd., Japan).

IPGTT. Mice fasted for 16–18 h were used. Body weights were measured. Blood glucose levels were measured before (0 min) or at 15 min, 30 min, 60 min, 90 min and 120 min after intraperitoneal administration of 25% Glucose (Sigma-Aldrich) solution at 2 g per kg body weight. Serum C-peptide concentrations were measured as described above.

Cell transplantation into AKITA mice. Differentiated cells were dissociated with 0.25% trypsin, resuspended in DMEM with 10% FBS and injected under the kidney capsules of AKITA mice (C57BL/6J-*Rag1*$^{-/-}$-*Ins2*$^{Akita/+}$; male)[27] with a 24G catheter (NIPRO, Japan). The AKITA mice were at least 6 weeks old. Six weeks after transplantation, the tissue was removed and analyzed for insulin expression, content and secretion, as described above.

Statistical tests. Data were analyzed by two-tailed *t*-test. Data are presented as mean ± s.d.

© 2014 Nature America, Inc. All rights reserved.

doi:10.1038/nchembio.1410

VMAT2 identified as a regulator of late-stage beta cell differentiation

Daisuke Sakano, Nobuaki Shiraki, Kazuhide Kikawa, Taiji Yamazoe, Masateru Kataoka, Kahoko Umeda, Kimi Araki, Di Mao, Shirou Matsumoto, Naomi Nakagata, Olov Andersson, Didier Stainier, Fumio Endo, Kazuhiko Kume, Motonari Uesugi and Shoen Kume

Nature Chemical Biology: doi:10.1038/nchembio.1410

SUPPLEMENTARY RESULTS

Supplemental Figure 1. The effect of VMAT2 inhibitors

Reserpine and TBZ increased Insulin positive cells and *Ins1* expression level.

Insulin (Ins)+ cell numbers (black bars) and *Ins1* mRNA levels (gray bars) of reserpine (0.63μM) and TBZ (1.25μM) versus control, respectively, are shown. Fold increases in *Ins1* transcripts (gray bars), versus controls are shown. Cont: without chemicals; mean ± SD are shown (n = 3); significant difference between treatment and control at $*p < 0.05$ and $**p < 0.01$ are shown (two-tailed paired Student's *t*-test).

Supplemental Figure 2. The effect of MAO_B inhibitor.

MAOB inhibition decreased the effect of Reserpine for positive regulation of beta-cell differentiation. A monoamine oxidase inhibitor (MAO_{Bi}) counteracted the effect of reserpine: Ins+ (upper panel) or *Pdx1*/GFP+ (lower panel) cells. Cont: without chemicals; mean ± SD are shown (n = 3); significant difference between treatment and control at $**p < 0.01$ are shown (two-tailed paired Student's *t*-test).

Supplemental Figure 3. Cellular contents of adrenaline and noradrenaline

VMAT2 decreased but MAO_{Bi} increased the cellular contents of adrenaline and noradrenaline. (a, b) Cellular contents of adrenaline (a), and noradrenaline (b) when added with VMAT2 inhibitors or MAO_{Bi}, treatment with both TBZ and dBu-c AMP, were determined, and normalized by their DNA contents (pg/μg DNA). Mean ± SD are shown (n = 3); significant difference between treatment and control were $*p < 0.05$ or $**p < 0.01$ (two-tailed paired Student's *t*-test), and are indicated above each bars.

Nature Chemical Biology: doi:10.1038/nchembio.1410

Supplemental Figure 4. Dopamine, histamine and serotonin related signaling molecules and their functions. Monoamine synthesizing enzymes and receptors were expressed and inhibiting their synthesis increased Ins+ cell numbers. (a-f) Quantitative PCR on d0- d15 differentiated ES cells, for the expression of the synthesizing enzymes *Th*, involved in the synthesis of dopamine (a), *Hdc,* for histamine (b) or *Tph1*, for serotonin (c), expressions of monoamine receptors, *Drd2* (d), *Hrh1* (e, black bars), *Hrh2* (e, grey bar), and *Htr1a* (f) in differentiated ES cells on d0, d11, and d13, are shown. Black or grey bars indicate expression levels, fold changes versus that expressed in d0 ES cells (a-c), or versus that in d11 ES cells (d-f) are shown. Expression levels in E16.5 pancreas buds are indicated as references in (a-c).

(g-i) Addition of inhibitors for the synthesis of dopamine with α-MT or L-DOPA (g), histamine with αFMH (h), or serotonin with 5HTP or carbidopa (i), enhanced differentiation of ES cells into Ins+ cells. Black bars indicate Ins+ cell numbers (fold change) relative to control. Mean ± SD are shown (n = 3 or 4); significant differences between treatment and control were $*p < 0.05$ or $**p < 0.01$ (two-tailed paired Student's *t*-test), and are indicated above each bars.

Nature Chemical Biology: doi:10.1038/nchembio.1410

Supplementary Figure 5. The effect of TBZ on Ngn3+ cells

The increase in Ngn3 cells by TBZ was not due to increased proliferation, or differential expressions of Nkx2.2, Nkx6.1 genes. (a) A representative fluorescence image (left panel) and quantitative representation (right panel) of EdU+ proliferative cells (red) within *Ngn3*/GFP- or *Ngn3*/GFP+ cells (green) cells, with or w/o TBZ. (b) Representative fluorescence images on day 13 of Ngn3/GFP cells (green) that co-expressed Nkx2.2 (upper panels) or Nkx6.1 (lower panels) in their nuclei, in untreated control (No chem. control, left) or cells treated with TBZ (TBZ, right). For observation in single cells, cells were dissociated and replated for 30min.

Nature Chemical Biology: doi:10.1038/nchembio.1410

Supplementary Figure 6. Expressions of mature endocrine, exocrine and duct markers in ES-derived beta cells on d17.

TBZ and dBu-cAMP did not change the maturation markers of the endocrine or exocrine. The exocrine cells did not appear in the ES cell culture.

(a, b) Beta cells treated with TBZ alone, dBu-cAMP alone or TBZ/dBu-dAMP were analyzed for their expressions of insulin (Ins, green) with (a) mature endocrine markers (red), Nkx2.2, Nkx6.1 and MafA, or (b) exocrine marker, Amylase (red), and a duct marker, *Dolichos biflorus* agglutinin (DBA) lectin (red). Ins (green) stainings were not observed in DBA+ cells. No Amy+ cells were observed. Adult pancreas served as positive controls for the stainings. (c) Ins+ cells that also co-expressed other endocrine hormones were calculated and shown as relative cell number (left panel), right panels show representative images of each type of cells. Yellow: cell co-expressed Ins with Gcg, SS and PP. Light blue, cells co-expressed Ins with SS and PP. Blue, cells co-expressed Ins with Gcg. Green, Ins single positive cells. The total number of endocrine hormones-positive cells in control condition is showed as 1.

Nature Chemical Biology: doi:10.1038/nchembio.1410

Supplementary Figure 7. The effects of TBZ and dBu-cAMP on insulin contents, and GSIS.

TBZ was effective to increase insulin contents and dBu-cAMP potentiates GSIS of the ES cells. (a) The net recovery in insulin contents from total cells treated with TBZ, dBu-cAMP, or both compounds were measured at a per well basis (left column), or per μg DNA basis (middle column). Fold changes (right column) are shown for the chemicals versus control (normalized with DNA contents). TBZ was more potent than dBu-cAMP in increasing C-peptide contents of the ES cells. (b) dBu-cAMP was potent in enhancing GSIS activity from d15, compared to controls with no chemicals. Gray bars, low glucose (5.5mM); black bars: high glucose (27.5 mM). Significant differences between treatment and control were $^{**}p < 0.01$ (two-tailed unpaired Student's *t*-test), and are indicated above each bars.

Nature Chemical Biology: doi:10.1038/nchembio.1410

Supplementary Figure 8. Time dependent effects of dBu-cAMP on beta cell differentiation into cells with GSIS ability.

VMAT2 inhibition showed no effects, but dBu-cAMP increased GSIS ability at late stages. (a) Upper panel, experimental procedure is shown. ES cells differentiated with no chemicals (untreated; doted white bar), with TBZ alone (dotted black bar) or with dBu-cAMP alone (shaded bar) during d11-15 or d11-17 were assayed for GSIS on d17 of differentiation, at conditions w/wo dBu-cAMP. (b) Secreted C-peptide level (ng mg protein $^{-1}$ hr $^{-1}$) at low (gray bars: 5.5 mM) or high (black bars: 27.5mM) glucose were measured. Longer exposure to dBu-cAMP during differentiation yielded beta cells with significantly higher GSIS ability. Significant difference between treatment and control were $^{*}p < 0.05$ or $^{**}p < 0.01$ (two-tailed paired Student's *t*-test), and are indicated above each bars.

Supplementary Figure 9. Insulin potentiated differentiation into insulin+ cells.

Insulin concentration in medium III at late stage dose dependently increases transcript level of itself.

Nature Chemical Biology: doi:10.1038/nchembio.1410

Supplementary Figure 10. The transplanted cells reversed hyperglycemia in diabetic mice.

The transplanted differentiated cells decreased fasting blood glucose levels, and increased serum insulin levels in the AKITA mice. (a) Fasting blood glucose levels of mice transplanted with TBZ/dBu-cAMP treated cells at 4×10^6 (red triangles), 1×10^7 (blue squares) or non-transplanted sham-operation controls (black circles). X axis: weeks after transplantation. (b) Serum C-peptide concentrations were measured at each time points after challenged with glucose. (c) Six weeks after transplantation, engrafted ES cell-derived cells were recovered and revealed no tumor formation (upper left panel, bright field), and immunohistochemical analysis (upper right, low magnification; middle panels, high magnifications) revealed that they were positive for insulin (Ins, red), but not glucagon (Gcg, yellow), pancreatic polypeptide (PP, yellow) or somatostatin (Sst, yellow). Normal adult islets were used as controls for immunohistochemical analyses (bottom panels). (d) After 6 weeks engraftment, recipient AKITA mice grafted with ES cell-derived cells were analyzed for their beta cell mass (% insulin+ cell). Upper panels: images of representative islets from control wild type (WT) (left); AKITA that were not grafted (middle); AKITA grafted with $4X10^6$ or $1X10^7$ ES cells treated with TBZ and dBu-cAMP (right). Note that the allocations of Ins+ cells (red) and glucagon (Gcg, yellow) are different from that of the control. Lower panel shows quantification of the ratios of beta cell number versus the whole pancreas. Significant difference between treatments and control were $^*p < 0.05$ or $^{**}p < 0.01$ (two-tailed unpaired Student's t-test), and are indicated above each bars.

Nature Chemical Biology: doi:10.1038/nchembio.1410